ELSEVIER

Journal of Organometallic Chemistry 517 (1996) 173–181

Journal of Organometallic Chemistry

The photochemical reactivity of triosmium cluster complexes containing 2-mercaptopyridine ligands: the crystal and molecular structures of the linked clusters $[\{Os_3H(CO)_{10}\}_2(\mu\text{-}SC_5H_3NCO_2)]$ and $[\{Os_3H(CO)_9\}(\mu\text{-}SC_5H_3NCO_2)\{Os_3H(CO)_{10}\}]$

Eric W. Ainscough [a,*], Andrew M. Brodie [a,*], Richard K. Coll [a], Thomas G. Kotch [b], Alistair J. Lees [b], Angelika J.A. Mair [a], Joyce M. Waters [a]

[a] *Department of Chemistry, Massey University, Palmerston North, New Zealand*

[b] *Department of Chemistry, State University of New York at Binghamton, Binghamton, NY 13902-6016, USA*

Received 15 November 1995

Abstract

The 2-mercaptopyridine triosmium cluster complexes, $[\{Os_3H(CO)_{10}\}_2(\mu\text{-}SC_5H_3NCO_2)]$, $[Os_3H(CO)_{10}\{SC_5H_3N(OH)\}]$ and $[Os_3H(CO)_{10}(SC_5H_4N)]$ upon exposure to irradiation at 366 nm undergo photochemical decarbonylation reactions in which the nitrogen of the mercaptopyridine ligand displaces a carbonyl on the third osmium of the thiolate-bridged triangle to yield $[\{Os_3H(CO)_9\}(\mu\text{-}SC_5H_3NCO_2)\{Os_3H(CO)_{10}\}]$, $[Os_3H(CO)_9\{SC_5H_3N(OH)\}]$ and $[Os_3H(CO)_9(SC_5H_4N)]$. The reactions proceed cleanly and quantum yields have been determined. The clusters have been characterised by spectroscopic means and the structures of $[\{Os_3H(CO)_{10}\}_2(\mu\text{-}SC_5H_3NCO_2)]$ and $[\{Os_3H(CO)_9\}(\mu\text{-}SC_5H_3NCO_2)\{Os_3H(CO)_{10}\}]$ established by single-crystal X-ray analyses. In both structures the osmiums form two triangles, with the carboxylate bridging one edge of one triangle and the sulphur that of a second. For $[\{Os_3H(CO)_9\}(\mu\text{-}SC_5H_3NCO_2)\{Os_3H(CO)_{10}\}]$ the nitrogen has displaced a carbonyl from the third osmium of the thiolate-bridged osmium triangle.

Keywords: Osmium cluster; Photochemistrv; Crystal structure; Thiolato

1. Introduction

Decarbonylation via thermolysis commonly occurs for triosmium carbonyl clusters [1–5]. For example, clusters of the form $[Os_3H(CO)_9L]$ (L = heterocyclic thioamide) are obtained from the decacarbonyl clusters $[Os_3H(CO)_{10}L]$ when refluxed in octane [2]. Similar reactions have been reported for triosmium clusters containing substituted pyridine ligands [1]. Thermolysis can lead to a mixture of products and difficulty may be encountered in controlling the extent of decarbonylation; however, controlled decarbonylation can be achieved by the use of trimethylamine oxide [2]. Less is known about decarbonylation by photochemical means [6]. Hence in this paper we report the photochemical decarbonylation of 2-mercaptopyridine triosmium clusters in which a single carbonyl group is lost from one of the osmium triangles. The reactions lead to one main product, allowing quantum yields to be determined, and provide useful synthetic routes for the formation of new cluster compounds. For the linked cluster $[\{Os_3H(CO)_{10}\}_2(\mu\text{-}SC_5H_3NCO_2)]$ and its corresponding photochemical reaction product $[\{Os_3H(CO)_9\}(\mu\text{-}SC_5H_3NCO_2)\{Os_3H(CO)_{10}\}]$, molecular structures have been determined by single-crystal X-ray analyses.

2. Results and discussion

Triangular triosmium clusters containing the deprotonated ligands 3-carboxy-2-mercaptopyridine $[\{Os_3H(CO)_{10}\}_2(\mu\text{-}SC_5H_3NCO_2)]$ (**1**), 3-hydroxo-2-mercaptopyridine $[Os_3H(CO)_{10}\{SC_5H_3N(OH)\}]$ (**2**), and 2-mercaptopyridine $[Os_3H(CO)_{10}(SC_5H_4N)]$ (**3**) when ir-

* Corresponding authors.

PII S0022-328X(96)06186-4

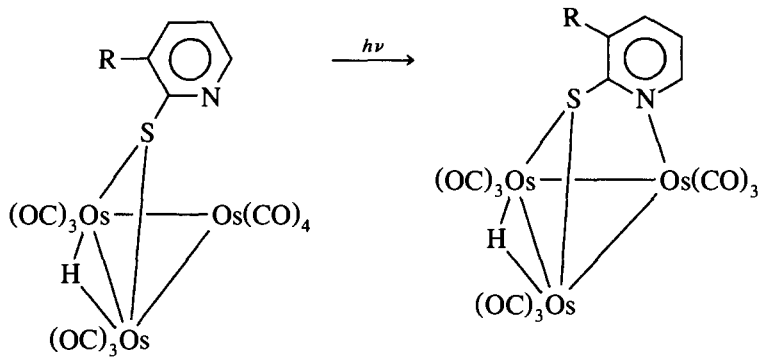

Scheme 1. Photochemical decarbonylation. For **1** and **4**, R = $\{Os_3H(CO)_{10}\}O_2C$; for **2** and **5**, R = OH; for **3** and **6**, R = H.

radiated with a tungsten lamp for short times (ca. 10 min) produce the decarbonylated products $[\{Os_3H(CO)_9\}(\mu\text{-}SC_5H_3NCO_2)\{Os_3H(CO)_{10}\}]$ (**4**), $[Os_3H(CO)_9\{SC_5H_3N(OH)\}]$ (**5**) and $[Os_3H(CO)_9(SC_5H_4N)]$ (**6**) respectively; in these reactions the nitrogen atom of the mercaptopyridine replaces the carbonyl group of the third osmium on the thiolate-bridged osmium triangle (see Scheme 1). Reaction also proceeds under the influence of sunlight but takes longer (ca. 4 h). Compounds have been characterized by spectroscopic methods (Table 1) and elemental analysis. Experimental mass spectra closely matched simulated spectra. The IR spectra of the linked clusters, **1** and **4**, show a complex pattern of carbonyl stretching bands consistent with the presence of both thiolate and carboxylate bridges. In **1**, for example, the highest frequency band at 2114 cm^{-1} is assignable to the carboxylate-bridged triosmium cluster and the band at 2107 cm^{-1} to the thiolate cluster. Similarly for **4**, the 2115 cm^{-1} band belongs to the carboxylate cluster and that at 2086 cm^{-1} to the thiolate. As can be seen, there are significant differences in the IR spectra in the ν(CO) region for the products in comparison with the starting materials, with the appearance of peaks characteristic of a nonacarbonyl-triosmium cluster in the former [6]. In particular, the disappearance of the band at ca. 2107 cm^{-1} and the appearance of the band at ca. 2086 cm^{-1} is a convenient indicator of the conversion. In addition, the hydride region of the ^1H NMR spectra shows significant changes with the resonances at ca. −17 ppm being replaced by new resonances at ca. −15 ppm. The linked clusters, **1** and **4**, show an additional resonance near −10 ppm assignable to the hydride trans to the carboxylate three atom bridge.

2.1. Photochemical studies

The photochemical conversions were carried out in dichloromethane for **1** and cyclohexane for **2** and **3**. In each instance the reactions were monitored by the disappearance of the high-energy absorption feature in the UV–vis spectrum. (Fig. 1). The observed UV–vis progressions show sharp isosbestic points, suggesting that the reactions proceed cleanly without interference from secondary photoprocesses or thermal decomposition. Quantum yields Φ at 293 K have been determined at an irradiating wavelength of 366 nm with incident light intensity of 1.32×10^{-5} einstein dm^{-3} s^{-1} (determined by ferrioxalate actinometry) (Table 2). Values of 0.043 and 0.060 (average of three measurements) were ob-

Table 1
Spectroscopic data for the complexes

Complex	$m/z[MH^+(^{192}Os)]$	$^1H(\delta)$[OsH] [a]	ν(CO) [b] (cm^{-1})
$[\{Os_3H(CO)_{10}\}_2(\mu\text{-}SC_5H_3NCO_2)]$ (**1**)	1867 [c]	−17.11, −10.05	2114w, 2107w, 2077s, 2069vs, 2057m, 2030m, 2022s, 2009s, 2003s, 1989m
$[Os_3H(CO)_{10}\{SC_5H_3N(OH)\}]$ (**2**)	984	−17.20	2108w, 2078vs, 2060s, 2023vs, 2013s, 2007s, 1991m, 1987m
$[Os_3H(CO)_{10}(SC_5H_4N)]$ (**3**) [d]		−17.09	2108w, 2068vs, 2058s, 2021s, 2014s, 2000s, 1983w
$[\{O_3H(CO)_9\}(\mu\text{-}SC_5H_3NCO_2)\{Os_3H(CO)_{10}\}]$ (**4**)	1840	−15.12, −10.42	2115w, 2086w, 2078s, 2064s, 2057s, 2030vs, 2022vs, 2012s, 2003s, 1989m, 1967w, 1953w.
$[Os_3H(CO)_9\{SC_5H_3N(OH)\}]$ (**5**)	956	−15.14	2087m, 2058vs, 2032vs, 2005vs 1991s, 1968w, 1956w
$[Os_3H(CO)_9(SC_5H_4N)]$ (**6**)	940	−15.14	2086w, 2056vs, 2030vs, 2002s, 1990s, 1966w, 1952w

[a] In $CDCl_3$. [b] In cyclohexane. [c] $M^+(^{192}Os)$. [d] Data from Ref. [1].

Table 2
Photochemical data for the 366 nm irradiation of the complexes **1**, **2** and **3** at 293 K

Complex	ε_{366} (M^{-1} cm^{-1})	α [c] (min^{-1})	Φ
$[\{Os_3(CO)_{10}\}_2(\mu\text{-}SC_5H_3NCO_2)]$ (**1**) [a]	8.72×10^3	−0.055	0.008
$[Os_3H(CO)_{10}\{SC_5H_3N(OH)\}]$ (**2**) [b]	2.88×10^3	−0.132	0.043
$[Os_3H(CO)_{10}(SC_5H_4N)]$ (**3**) [b]	3.84×10^3	−0.182	0.060

[a] In CH_2Cl_2. [b] In cyclohexane. [c] $\alpha = -\Phi I_0 \varepsilon_R b$.

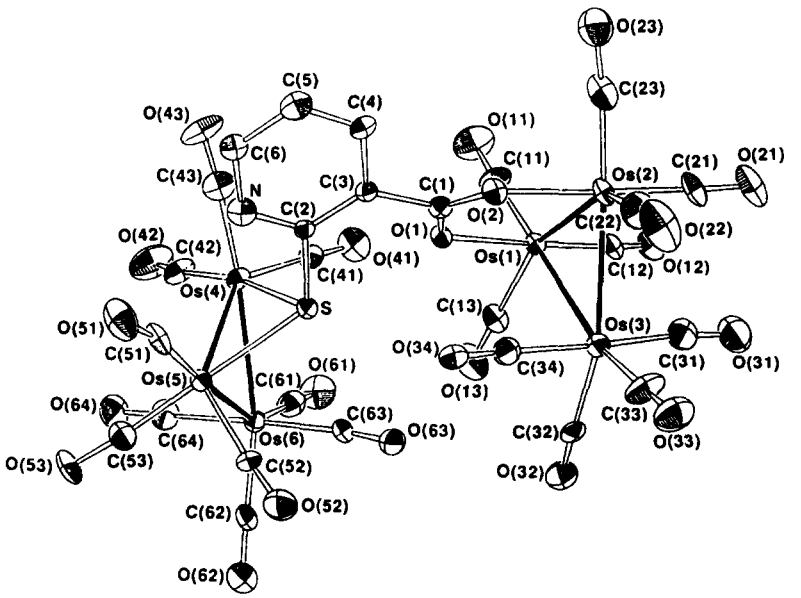

Fig. 2. ORTEP diagram of $[\{Os_3H(CO)_{10}\}_2(\mu\text{-}SC_5H_3NCO_2)]$ (**1**) showing the labelling scheme used. Ellipsoids are drawn at the 20% probability level; hydrogen atoms have been omitted for clarity.

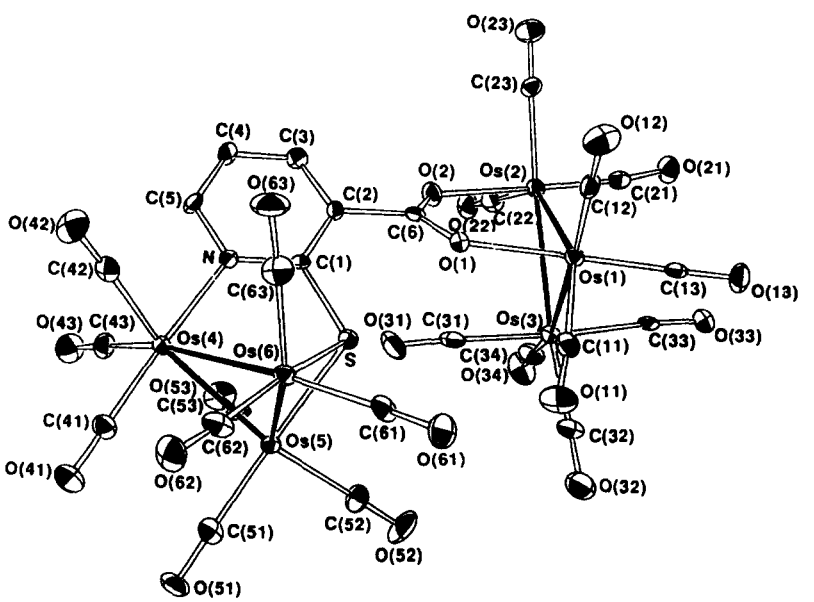

Fig. 3. ORTEP diagram of $[\{Os_3H(CO)_9\}(\mu\text{-}SC_5H_3NCO_2)\{Os_3H(CO)_{10}\}]$ (**4**) showing the labelling scheme used. Details as in Fig. 2.

Table 3
Selected bond lengths (Å) and angles (deg) for $[\{Os_3H(CO)_{10}\}_2(\mu\text{-}SC_5H_3NCO_2)]$ (**1**) with estimated standard deviations in parentheses

Os(1)–Os(2)	2.902(1)	Os(2)–O(2)	2.141(12)
Os(1)–Os(3)	2.869(1)	O(1)–C(1)	1.28(2)
Os(2)–Os(3)	2.869(1)	O(2)–C(1)	1.26(2)
Os(1)–O(1)	2.172(12)	C(1)–C(3)	1.50(2)
Os(4)–Os(5)	2.862(1)	Os(5)–S	2.412(4)
Os(4)–Os(6)	2.849(1)	S–C(2)	1.80(1)
Os(5)–Os(6)	2.850(1)	N–C(2)	1.28(2)
Os(4)–S	2.400(4)	N–C(6)	1.40(2)
Os(2)–Os(1)–Os(3)	59.6(0)	Os(1)–Os(2)–Os(3)	59.6(0)
Os(1)–Os(3)–Os(2)	60.8(0)	O(1)–Os(1)–Os(2)	82.1(3)
O(1)–Os(1)–Os(3)	91.2(3)	O(2)–Os(2)–Os(1)	81.5(3)
O(2)–Os(2)–Os(3)	92.0(3)	Os(1)–O(1)–C(1)	121.7(10)
Os(2)–O(2)–C(1)	125(1)	O(1)–C(1)–O(2)	129(2)
O(1)–C(1)–C(3)	116(1)	O(2)–C(1)–C(3)	115(1)
Os(5)–Os(4)–Os(6)	59.9(0)	Os(4)–Os(5)–Os(6)	59.8(0)
Os(4)–Os(6)–Os(5)	60.3(0)	S–Os(4)–Os(5)	53.7(1)
S–Os(4)–Os(6)	80.9(1)	S–Os(5)–Os(4)	53.3(1)
Os(4)–S–C(2)	106.3(5)	Os(5)–S–C(2)	111.7(6)
S–C(2)–N	117(1)	S–C(2)–C(3)	120(1)
N–C(2)–C(3)	124(1)	C(2)–N–C(6)	119(2)

served for the compounds $[Os_3H(CO)_{10}\{SC_5H_3N(OH)\}]$ (**2**) and $[Os_3H(CO)_{10}(SC_5H_4N)]$ (**3**) respectively, showing that both photoconversions proceed with relatively high efficiency. The values are greater than that of 0.008 found for the linked cluster $[\{Os_3H(CO)_{10}\}_2(\mu\text{-}SC_5H_3NCO_2)]$ (**1**), possibly due to the increased size of the latter giving rise to a larger number of non-radiative decay routes. The quantum yields for **2** and **3** are

Table 4
Selected bond lengths (Å) and angles (deg) for $[\{Os_3H(CO)_9\}(\mu\text{-}SC_5H_3NCO_2)\{Os_3H(CO)_{10}\}] \cdot CH_3CO_2CH_2CH_3$ (**4**) with estimated standard deviations in parentheses

Os(1)–Os(2)	2.936(1)	Os(2)–O(2)	2.144(9)
Os(1)–Os(3)	2.876(1)	O(1)–C(6)	1.28(2)
Os(2)–Os(3)	2.861(1)	O(2)–C(6)	1.27(2)
Os(1)–O(1)	2.119(8)	C(6)–C(2)	1.53(2)
Os(4)–Os(5)	2.800(1)	Os(4)–N	2.188(10)
Os(4)–Os(6)	2.796(1)	S–C(1)	1.792(14)
Os(5)–Os(6)	2.853(1)	N–C(1)	1.35(2)
Os(5)–S	2.417(4)	N–C(5)	1.35(2)
Os(6)–S	2.420(4)		
Os(2)–Os(1)–Os(3)	59.0(0)	Os(1)–Os(2)–Os(3)	59.5(0)
Os(1)–Os(3)–Os(2)	61.6(0)	O(1)–Os(1)–Os(2)	80.6(3)
O(1)–Os(1)–Os(3)	92.9(3)	O(2)–Os(2)–Os(1)	81.2(3)
O(2)–Os(2)–Os(3)	90.9(3)	Os(1)–O(1)–C(6)	127.0(8)
Os(2)–O(2)–C(6)	125.1(8)	O(1)–C(6)–O(2)	125.7(12)
O(1)–C(6)–C(2)	117.9(11)	O(2)–C(6)–C(2)	116.3(10)
Os(5)–Os(4)–Os(6)	61.3(0)	Os(4)–Os(5)–Os(6)	59.3(0)
Os(4)–Os(6)–Os(5)	59.4(0)	S–Os(5)–Os(4)	80.4(1)
S–Os(5)–Os(6)	53.9(1)	S–Os(6)–Os(4)	80.5(1)
S–Os(6)–Os(5)	53.8(1)	Os(5)–S–Os(6)	72.3(1)
Os(5)–S–C(1)	105.5(4)	Os(6)–S–C(1)	108.9(5)
Os(5)–Os(4)–N	86.8(4)	Os(6)–Os(4)–N	87.5(3)
Os(4)–N–C(1)	124.5(9)	Os(4)–N–C(5)	117.3(8)
S–C(1)–N	115.9(9)	S–C(1)–C(2)	123.3(10)

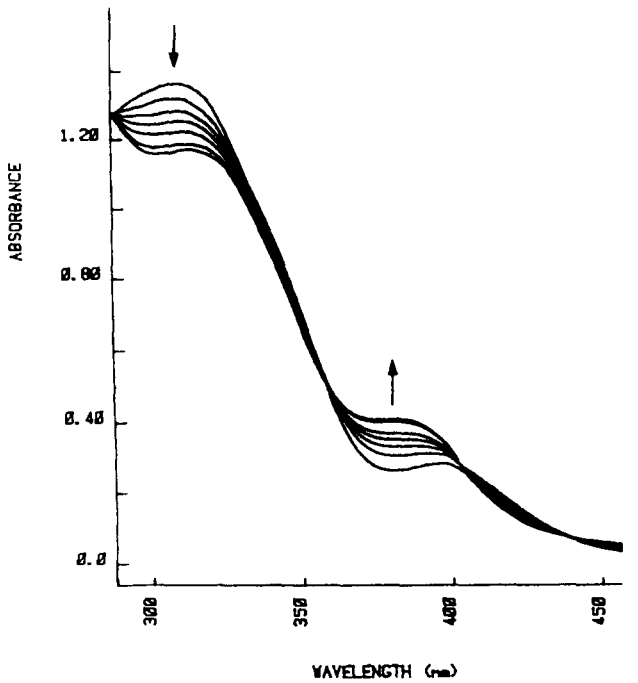

Fig. 1. UV–vis changes accompanying the 366 nm photolysis of $[Os_3H(CO)_{10}\{SC_5H_3N(OH)\}]$ (**2**) in deoxygenated cyclohexane at 293 K. Spectra recorded at 30 s photolysis intervals; initial spectrum recorded prior to photolysis.

similar to those previously reported [6] for similar photochemical decarbonylation reactions of the phenylthioureato complexes $[Os_3H(CO)_{10}L]$ [L = SC(NPh)(NHPh) or SC(NPh)(NH_2)]. For these complexes it was suggested that the initial step of carbonyl dissociation occurred from a ligand field type) (or d–d type) excited state. Such excited states often undergo facile ligand dissociation with low activation energy barriers [7].

2.2. Structures of $[\{Os_3H(CO)_{10}\}_2(\mu\text{-}SC_5H_3NCO_2)]$ (1) and $[\{Os_3H(CO)_9\}(\mu\text{-}SC_5H_3NCO_2)\{Os_3H(CO)_{10}\}] \cdot CH_3CO_2CH_2CH_3$ (4)

These molecular structures are shown in Figs. 2 and 3. Selected bond lengths and angles are given in Tables 3 and 4. For **1** the osmium atoms form two triangles with the carboxylate bridging one edge of one triangle and the sulphur that of a second. The structure of **4** is similar to that of **1** except that the ligand nitrogen has displaced a carbonyl group from the third osmium of one triangle. In both structures the Os–Os bond lengths for the osmium atoms which are bridged by the carboxylate group are longer compared with others in the same triangle (2.902(1), 2.936(1) Å cf. 2.861(1)–2.876(1) Å) as has been observed previously [8–12]. However, this effect is sensitive to the coordination around the osmiums and may vary when carbonyls are replaced by other donor atoms. For the osmium triangles containing a thiolate bridge, the Os–Os bond length of the osmium atoms bridged by the sulphur atom is also longer than those found between the other osmiums in the same triangle (2.862(1), 2.853(1) Å cf. 2.850(1)–2.796(1) Å). This result is the same as observed for the unsubstituted 2-pyridinethiolato complex, $[Os_3H(CO)_9(SC_5H_4N)]$ [5], but there is not a consistent trend for other μ-S clusters [13–17]. The Os–O distances (2.119(8)–2.172(12) Å) and Os–S distances (2.400(4)–2.420(4) Å) are similar to reported values [5,6,8–17], but the Os–N distance (2.188(10) Å) is at the upper end of the range observed for similar structures (2.058(9)–2.19(1) Å) [5,6,17–19]. This latter distance is influenced by the difference in coordination around the osmium atoms; however, it is noted that long Os–N bond lengths have been found in structures in which the nitrogen is multiply bonded to an adjacent carbon [15]. The C–O distances for the carbonyls and C–C distances for the ligands are similar to reported values [8–20].

3. Experimental

Infrared spectra were recorded as solutions using 0.5 mm NaCl cells on a BIO-RAD FTS-40 spectrometer. Mass spectra were recorded by the liquid secondary ion mass spectroscopy (LSIMS) technique using a Varian VG70-250S mass spectrometer from samples in a *m*-nitrobenzyl alcohol matrix. ^{1}H NMR spectra were recorded on a Jeol GX270W spectrometer. Elemental analyses were determined at the Campbell Microanalytical Laboratory, University of Otago. All solvents were dried by distillation over calcium hydride and all reactions, but not work up, carried out under an atmosphere of dry dioxygen-free dinitrogen. The starting complex $[Os_3(CO)_{10}(MeCN)_2]$ was prepared from $[Os_3(CO)_{12}]$ according to a literature method [21]. The reaction products were purified by thin layer chromatography (TLC) using plates coated with 2 mm of Merck Kieselgel 60 PF_{254} silica gel and elution with hexane–CH_2Cl_2 mixtures. Yields were typically in the range 70–90%.

3.1. Syntheses

$[\{Os_3H(CO)_{10}\}_2(\mu\text{-}SC_5H_3NCO_2)]$ (**1**). The complex $[Os_3(CO)_{10}(MeCN)_2]$ (40 mg, 0.043 mmol) was stirred with 0.5 equivalent of 3-carboxy-2-mercaptopyridine, in CH_2Cl_2 (20 cm^3) and stirred at room temperature for 1 h. The solvent was removed under reduced pressure and the product purified by TLC to yield yellow microcrystals. (Found: C, 16.95; H, 0.30; N, 0.71. $C_{26}H_5NO_{22}Os_6S$. Calc.: C, 16.82; H, 0.27; N, 0.75%.)

$[Os_3H(CO)_{10}\{SC_5H_3N(OH)\}]$ (**2**). This was prepared in a manner similar to that described above for **1** using 1 equivalent of the ligand 3-hydroxo-2-mercaptopyridine, and stirring for 10 min. (Found: C, 18.51; H, 0.54;

N, 1.40. $C_{15}H_5NO_{11}Os_3S$. Calc.: C, 18.43; H, 0.52; N, 1.43%.)

$[Os_3H(CO)_{10}(SC_5H_4N)]$ (**3**). This was prepared in a manner similar to that described above for **2** using 1 equivalent of the ligand 2-mercaptopyridine. The product was identified by comparison with previously reported spectroscopic data [1].

$[\{Os_3H(CO)_9\}(\mu\text{-}SC_5H_3NCO_2)\{Os_3H(CO)_{10}\}]$ (**4**). A CH_2Cl_2 solution of **1** was irradiated for 8 min (150 W tungsten lamp). The reaction was monitored by IR spectroscopy in the ν(CO) region and irradiation stopped when absorbances due to **1** were no longer identifiable. The solvent was removed under reduced pressure and the product purified by TLC to yield orange microcrystals. (Found: C; 16.60; H, 0.32; N, 0.72. $C_{25}H_5NO_{21}Os_6S$. Calc.: C, 16.42; H, 0.28; N, 0.77%.)

$[Os_3H(CO)_9\{SC_5H_3N(OH)\}]$ (**5**). This was prepared, in a manner similar to **4** above from **2**, as orange microcrystals. (Found: C, 17.90; H, 0.56; N, 1.40. $C_{14}H_5NO_{10}Os_3S$. Calc.: C, 17.71; H, 0.53; N, 1.48%.)

$[Os_3H(CO)_9(SC_5H_4N)]$ (**6**). This was prepared from **3** in a manner similar to that described for **5** and identified spectroscopically by comparison with reported literature data for the complex prepared thermally [1].

3.2. Photolysis experiments

Photolysis experiments at 366 nm were preformed with an Ealing Corporation 200 W medium-pressure mercury lamp using an interference filter (bandpass 10 nm) to isolate the excitation wavelength. Solutions were filtered through a 0.22 μm Millipore filter, deoxygenated by purging with purified dinitrogen and maintained at 20°C prior to irradiation. In all photolysis experiments the concentrations of reactant and product were monitored throughout the reaction by recording UV–vis and FTIR spectra on Hewlett-Packard 8450A UV–vis and Nicolet 20 SXC FTIR spectrophotometers respectively. During photolysis samples were stirred to ensure homogeneous light absorption by the solution. Incident light intensities at 366 nm were determined by ferrioxalate actinometry [22].

Photochemical quantum yields Φ were determined by monitoring the disappearance of the reactant complexes at their respective absorption maxima and by

Table 5
Crystallographic data [a] for $[\{Os_3H(CO)_{10}\}_2(\mu\text{-}SC_5H_3NCO_2)]$ (**1**) and $[\{Os_3H(CO)_{10}\}(\mu\text{-}SC_5H_3NCO_2)\{Os_3(CO)_9\}]\cdot CH_3CO_2CH_2CH_3$ (**4**)

Compound	**1**	**4**
Formula	$C_{26}H_5NO_{22}Os_6S$	$C_{29}H_{13}NO_{23}Os_6S$
M	1856.58	1916.68
Colour	yellow	orange
Crystal size (mm^3)	0.25 × 0.23 × 0.05	0.25 × 0.12 × 0.05
Crystal system	triclinic	triclinic
Space group	$P\bar{1}$ (no. 2)	$P\bar{1}$ (no. 2)
a (Å)	9.689(2)	14.162(1)
b (Å)	13.767(4)	16.068(2)
c (Å)	15.297(4)	9.934(1)
α (deg)	95.69(2)	105.406(9)
β (deg)	87.28(2)	112.063(9)
γ (deg)	101.98(2)	84.401(9)
U (Å^3)	1985.3(8)	2019.6(4)
Z	2	2
D_c (g cm^{-3})	3.01	3.15
μ(Mo K α) (cm^{-1})	192.8	189.5
F(000)	1632	1700
Total data	7420	7360
Unique data	6253	6336
Data with $I_0 > 3.0\sigma(I_0)$	4800	4767
Scan range (deg)	1.10 + 0.34 tan θ	0.80 + 0.34 tan θ
Aperture-horizontal (mm)	1.60 + 0.80 tan θ	1.6 + 1.0 tan θ
Aperture-vertical (mm)	4	4
θ range (deg)	2–25	2–25
Parameters refined	505	511
R [b]	0.0460	0.0307
R_w	0.0544	0.0345
k	0.3023	0.8358
g	0.020854	0.001868

[a] Details in common: scan type ω–2θ maximum scan time per reflection 60 s; pre-scan speed 20 deg min^{-1}; pre-scan acceptance criterion $\sigma(I)/I < 0.66$; required $\sigma(I)/I < 0.02$; function minimised $\Sigma w(|F_0| - |F_c|)^2$ where $w = k/[\sigma^2(F) + gF^2]$.
[b] $R = [\Sigma|(|F_0| - k|F_c|)|/\Sigma|F_0|]$, $R_w = [\Sigma w(|F_0| - |F_c|)^2/\Sigma w|F_0|^2]$.

application of Eq. (1) which accounts for the changing degree of light absorption and for inner-filter effects.

$$d[R]/dt = -\Phi I_0(1-10^{-D})\varepsilon_R b[R]/D \quad (1)$$

Here, [R] is the concentration of the reactant complex at varying photolysis time t, I_0 is the intensity of the incident light per unit solution volume, ε_R and D are the molar absorption coefficients of the reactant complex and the solution optical density at the photolysis wavelength respectively, b is the cell path length and Φ is the reaction quantum yield. Plots of $\ln[(D_t - D_\infty)/(D_0 - D_\infty)]$ vs. $\int_{t_0}^{t}[(1-10^{-D})/D]\,dt$, where D_t, D_∞ and D_0 are the optical densities throughout the photolysis sequence at the reactant's absorption maximum gave straight lines of slope equal to $-\Phi I_0 \varepsilon_R b$. Obtained quantum yields were found to be reproducible to within 10%.

3.3. Molecular structure determination of [{$Os_3H(CO)_{10}$}$_2$(μ-$SC_5H_3NCO_2$)] (1) and [{$Os_3H(CO)_9$}(μ-$SC_5H_3NCO_2$){$Os_3H(CO)_{10}$}] · $CH_3CO_2CH_2CH_3$ (4)

Single crystals suitable for X-ray diffraction were obtained by the slow evaporation of a chloroform solution for **1** and by solvent diffusion (ethylacetate–methanol) for **4**. The crystal data, data collection and structure solution details are given in Table 5. The unit cell parameters were determined by the least squares refinement of 22 accurately centred reflections in the shell $8 < \theta < 15°$ for **1** and 25 reflections in the shell $12 < \theta < 15°$ for **4**. The data were collected at room temperature using an Enraf–Nonius CAD4 diffractometer with graphite-monochromated Mo Kα radiation (λ = 0.71073 Å) in the ω–2θ mode with $2 < \theta < 25°$ ($+h, \pm k, \pm l$) for **1** and $2 < \theta < 25°$ ($\pm h, +k, \pm l$) for **4**. Reflection intensities were corrected for the effects of Lorentz and polarisation effects and the crystal stability monitored two-hourly by observation of three standard reflections. Crystal decay was linear (16.2%, 2.3% for **1** and **4** respectively) and the data were scaled accordingly. Empirical absorption corrections were based on azimuthal scans (minimum, maximum transmission 0.4859, 0.9987 and 0.6392, 0.9995 for **1** and **4** respectively). A total of 6253 and 6336 unique data were recorded for **1** and **4** respectively (R merging 0.032, 0.017 for the two data sets respectively).

The structures were solved by the heavy atom method after location of the osmium atoms from the Patterson map. Refinement of the structures was carried out by the full-matrix least squares technique. Atomic scattering factors were taken from Ref. [23] and corrected for anomalous scattering using values from Ref. [24]. All non-hydrogen atoms were modelled assuming anisotropic thermal motion. Hydrogen atoms for the ligands were added in calculated positions (C–H = 0.96 Å) and refined riding on their corresponding carbons; a single fixed thermal parameter ($U = 0.06$) was used. The bridging hydrides were not located. For **4**, evidence was found for an ethylacetate solvent molecule which was included in the model of the structure. (Two disordered

Table 6
Atom coordinates (10^4) for [{$Os_3H(CO)_{10}$}$_2$(μ-$SC_5H_3NCO_2$)] (**1**)

Atom	x	y	z
Os(1)	2038.7(.7)	1990.2(.5)	2093.3(.4)
Os(2)	4489.0(.8)	3198.4(.5)	2966.6(.5)
Os(3)	4811.7(.8)	2065.6(.6)	1318.6(.5)
Os(4)	−198.0(.7)	−1996.1(.6)	3228.5(.4)
Os(5)	2167.7(.8)	−2954.2(.5)	2957.1(.5)
Os(6)	404.9(.9)	−2887.8(.6)	1530.4(.4)
S	2232(4)	−1185(3)	3064(2)
O(1)	2360(11)	920(8)	2973(7)
O(2)	4258(12)	1906(9)	3674(7)
O(11)	−822(19)	1950(19)	2979(13)
O(12)	1397(18)	3490(13)	956(11)
O(13)	852(19)	265(14)	737(12)
O(21)	4811(20)	5048(12)	2064(15)
O(22)	7632(19)	3570(15)	3186(16)
O(23)	3852(25)	4238(17)	4727(14)
O(31)	4566(25)	3840(15)	288(15)
O(32)	3963(18)	638(14)	−325(9)
O(33)	8039(20)	2502(17)	1115(12)
O(34)	5150(15)	324(11)	2359(8)
O(41)	−1297(20)	−399(15)	2473(13)
O(42)	−3171(21)	−3250(22)	3292(14)
O(43)	−459(18)	−1276(18)	5172(9)
O(51)	3691(21)	−3148(13)	4609(12)
O(52)	4721(20)	−2720(14)	1741(13)
O(53)	1401(23)	−5215(11)	2663(13)
O(61)	−1875(22)	−2121(16)	691(12)
O(62)	1621(25)	−4179(15)	59(12)
O(63)	2777(16)	−1178(11)	983(9)
O(64)	−1644(25)	−4750(13)	2119(12)
N	2735(15)	−1171(13)	4743(10)
C(1)	3272(16)	1155(13)	3580(10)
C(2)	2766(15)	−598(12)	4132(9)
C(3)	3209(17)	416(13)	4249(10)
C(4)	3628(15)	854(14)	5099(9)
C(5)	3585(21)	250(18)	5750(12)
C(6)	3101(17)	−756(15)	5592(12)
C(11)	320(21)	1946(19)	2677(12)
C(12)	1723(21)	2965(13)	1355(13)
C(13)	1300(19)	920(15)	1244(14)
C(21)	4702(21)	4320(14)	2408(16)
C(22)	6469(27)	3447(22)	3134(17)
C(23)	4142(27)	3874(17)	4032(15)
C(31)	4628(27)	3182(20)	721(15)
C(32)	4290(18)	1119(15)	258(12)
C(33)	6763(23)	2336(22)	1147(14)
C(34)	4948(23)	949(17)	1975(13)
C(41)	−924(20)	−1012(15)	2759(11)
C(42)	−2027(18)	−2845(18)	3270(11)
C(43)	−350(19)	−1511(19)	4427(14)
C(51)	3164(22)	−2966(13)	4007(14)
C(52)	3736(24)	−2853(16)	2154(13)
C(53)	1701(25)	−4330(17)	2733(15)
C(61)	−1117(27)	−2475(19)	84(14)
C(62)	1147(27)	−3690(14)	633(13)
C(63)	1867(21)	−1758(14)	1197(12)
C(64)	−908(25)	−4069(18)	1903(14)

Table 7
Atom coordinates (10^4) and isotropic temperature factors (10^3) for $[\{Os_3H(CO)_{10}\}(\mu\text{-}SC_5H_3NCO_2)\{Os_3H(CO)_9\}]\cdot CH_3CO_2CH_2CH_3$ (4)

Atom	x	y	z	U
Os(1)	1827.3(.4)	1626.6(.3)	442.8(.6)	
Os(2)	1006.0(.4)	3335.2(.3)	1405.3(.6)	
Os(3)	1401.9(.4)	2099.7(.4)	3160.9(.7)	
Os(4)	7558.7(.4)	2787.9(.3)	5080.5(.6)	
Os(5)	6324.9(.4)	1822.6(.3)	5747.4(.7)	
Os(6)	6704.1(.4)	1246.3(.4)	3022.1(.7)	
S	5176(2)	1956(2)	3299(4)	
O(1)	3195(6)	2356(6)	1440(10)	
O(2)	2591(7)	3667(6)	2298(12)	
O(11)	3163(9)	146(8)	1454(16)	
O(12)	2092(11)	1386(8)	−2540(15)	
O(13)	−30(7)	474(7)	−1154(14)	
O(21)	−1261(7)	3042(7)	150(15)	
O(22)	840(10)	4747(9)	4045(16)	35(3)
O(23)	625(9)	4417(7)	−832(15)	
O(31)	3560(8)	2856(10)	4894(14)	
O(32)	2049(10)	408(9)	4130(15)	
O(33)	−806(8)	1414(7)	1435(13)	
O(34)	761(9)	3078(10)	5742(14)	
O(41)	9406(8)	1849(8)	6700(16)	
O(42)	8678(9)	3326(9)	3339(16)	
O(43)	8057(10)	4304(8)	7814(15)	
O(51)	8014(9)	1311(8)	8372(13)	
O(52)	4702(10)	830(9)	6005(18)	
O(53)	5963(10)	3553(8)	7617(15)	
O(61)	5660(10)	−484(7)	1124(14)	
O(62)	8836(8)	505(8)	3558(16)	
O(63)	6681(11)	2001(10)	491(15)	
N	6163(7)	3434(7)	3956(13)	
C(1)	5226(9)	3071(8)	3328(14)	
C(2)	4368(9)	3552(9)	2756(15)	
C(3)	4456(10)	4402(9)	2862(17)	
C(4)	5396(11)	4766(8)	3448(18)	
C(5)	6242(10)	4267(8)	3972(17)	
C(6)	3295(10)	3163(8)	2085(14)	
C(11)	2635(11)	684(10)	1041(17)	
C(12)	2018(11)	1470(9)	−1420(17)	
C(13)	652(10)	921(8)	−517(14)	
C(21)	−381(11)	3112(9)	653(17)	
C(22)	899(12)	4204(10)	3059(20)	
C(23)	788(10)	4022(9)	−35(17)	
C(31)	2758(11)	2582(10)	4203(18)	
C(32)	1784(13)	1035(11)	3761(18)	
C(33)	−10(10)	1678(9)	2022(17)	
C(34)	991(12)	2747(11)	4762(17)	
C(41)	8716(11)	2211(10)	6091(18)	
C(42)	8231(10)	3144(9)	3955(19)	
C(43)	7847(11)	3739(10)	6755(20)	
C(51)	7378(12)	1512(10)	7385(17)	
C(52)	5295(11)	1150(10)	5868(19)	
C(53)	6094(11)	2910(9)	6913(18)	
C(61)	6014(11)	156(9)	1803(16)	
C(62)	8017(13)	754(10)	3332(18)	
C(63)	6676(13)	1693(12)	1417(22)	
C(71)	4154(21)	2928(19)	8827(32)	113(9)
C(72)	3553(31)	3762(28)	8905(47)	192(14)
O(73)	2765(24)	3520(20)	9084(35)	253(12)
O(74)	2893(31)	4347(29)	7721(47)	344(17)
C(75)	2728(29)	5100(25)	8734(45)	145(12)
C(76)	1821(84)	5094(66)	7725	332(43)
C(77)	3052(87)	5682(82)	9957	378(52)

sites were indentified for the terminal C of the ethyl moiety.) There was also evidence for solvent in the structure of **1**; however, disorder associated with the molecule made clear identification impossible and it was not included in the final structural model. Atomic coordinates for the two structures are given in Tables 6 and 7.

The data were processed using the MolEN package [25] and structure solution and refinement calculations were carried out using the SHELX-76 and SHELXS-86 system of programs [26].

Additional material, available from the Cambridge Crystallographic Data Centre, comprises H-atom coordinates, and full lists of bond lengths and angles.

Acknowledgements

We acknowledge support from the New Zealand Lottery Grants Board, Massey University for Postdoctoral Fellowships (to R.K.C. and A.J.A.M) and the Division of Chemical Sciences, Office of Basic Energy Sciences, Office of Energy Research, US Department of Energy (Grant DE-FG02-89ER14039). We thank Mr J. Allen, Horticultural and Food Research Institute of New Zealand Ltd., for mass spectra.

References

[1] K. Burgess, B.F.G. Johnson and J. Lewis, *J. Organomet. Chem., 233* (1982) C55.
[2] A.M. Brodie, H.D. Holden, J. Lewis and M.J. Taylor, *J. Chem. Soc. Dalton Trans.*, (1986) 633.
[3] D.F. Shriver, H.D. Kaesz and R.D. Adams (eds.), *The Chemistry of Metal Cluster Complexes*, VCH, New York, 1990.
[4] K. Burgess, *Polyhedron, 3* (1984) 1175.
[5] A.J. Deeming, R. Vaish, A.J. Arce and Y. De Sanctis, *Polyhedron, 13* (1994) 3285.
[6] E.W. Ainscough, A.M. Brodie, S.L. Ingham, T.G. Kotch, A.J. Lees, J. Lewis and J.M. Waters, *J. Chem. Soc. Dalton Trans.*, (1994) 1.
[7] A.J. Lees, *Chem. Rev., 87* (1987) 711; G.L. Geoffroy and M.S. Wrighton, *Organometallic Photochemistry*, Academic Press, New York, 1979.
[8] J.R. Shapley, G.M. St. George, M.R. Churchill and F.J. Hollander, *Inorg. Chem., 21* (1982) 3295.
[9] B.F.G. Johnson, J. Lewis, P.R. Raithby, V.P. Saharan and W.T. Wong, *J. Chem. Soc. Chem. Commun.*, (1991) 365.
[10] V.D. Alexiev, J. Evans, A.C. Street and M. Webster, *Acta Crystallogr. Sect. C:, 44* (1988) 1186.
[11] P.M. Lausarot, G.A. Vaglio, M. Valle, A. Tiripicchio, M.T. Camellini and P. Gariboldi, *J. Organomet. Chem., 221* (1985) 291.
[12] M. Webster, A.C. Street, J. Evans and V.D. Alexiev, *Acta Crystallogr. Sect. C:, 46* (1990) 1843.
[13] V.F. Allen, R. Mason and P.B. Hitchcock, *J. Organomet. Chem., 140* (1977) 297.
[14] H.D. Holden, B.F.G. Johnson, J. Lewis, P.R. Raithby and G. Uden, *Acta Crystallogr. Sect. C:, 39* (1983) 1197; 1200; 1203.

[15] R.D. Adams and Z. Dawoodi, *J. Am. Chem. Soc., 103* (1981) 6510.
[16] R.D. Adams, N.M. Golembeski and J.P. Selegue, *J. Am. Chem. Soc., 103* (1981) 546.
[17] A.J. Deeming, R. Peters, M.B. Hursthouse and J.D.J. Backer-Dirks, *J. Chem. Soc. Dalton Trans.*, (1982) 787.
[18] K. Burgess, B.F.G. Johnson, J. Lewis and P.R. Raithby, *J. Chem. Soc. Dalton Trans.*, (1982) 2085.
[19] K. Burgess, H.D. Holden, B.F.G. Johnson and J. Lewis *J. Chem. Soc. Dalton Trans.*, (1983) 1199.
[20] C.H. MacGillavry and G.D. Rieck (eds.), *International Tables for X-ray Crystallography*, Vol. 3, Kynoch Press, Birmingham, 1962.
[21] S.R. Drake and R. Khattar, *Organomet. Synth., 4* (1988) 234.
[22] C.G. Hatchard and C.A. Parker, *Proc. R. Soc. London Ser. A:, 235* (1956) 518.
[23] D.T. Cromer and J.B. Mann, *Acta Crystallogr. Sect. A:, 24* (1968) 321.
[24] D.T. Cromer and D. Liberman, *J. Chem. Phys., 53* (1970) 1891.
[25] MolEN, *An interactive structure solution procedure*, 1990 (Enraf–Nonius, Delft, Netherlands).
[26] G.M. Sheldrick, *Programs for crystal structure determinations*, University of Cambridge.